Available online at www.sciencedirect.com
ScienceDirect
Journal of Power Sources 180 (2008) 103–113
JOURNAL OF POWER SOURCES
www.elsevier.com/locate/jpowsour

Some fundamental aspects in electrochemical hydrogen purification/compression

Cristina Casati [a], Paolo Longhi [a], Luciano Zanderighi [a,*], Fiorenzo Bianchi [b]

[a] *Department of Physical Chemistry and Electrochemistry, Via Golgi 19, 20133 Milano, Italy*
[b] *Department of Chemistry, Materials and Chemical Engineering Politecnico di Milano, Piazza Leonardo da Vinci 2, 20133 Milano, Italy*

Received 5 November 2007; received in revised form 17 December 2007; accepted 26 January 2008
Available online 23 February 2008

Abstract

The electrochemical concentration of hydrogen from a poor hydrogen–inert gas mixture has been investigated by means of an electrochemical cell similar in construction to a hydrogen–air fuel cell, hydrogen being transported as hydrated protons, thorough a Nafion membrane, from the inlet (anode) to the outlet (cathode) compartments of the cell. Galvanostatic and tensiostatic mode of operation have been investigated: in the first case and erratic behaviour of the cell has been observed, mainly because of the non-controllable variations of the membrane water content. Under tensiostatic condition the role of the applied voltage, feed flow rate, water vapour content in the feed mixture and temperature has been studied, with two different designs of the gas feed distribution plates. From the analysis of experimental data it is possible to evaluate the current efficiency, the hydrogen recovery, the hydrogen purity, the exergy gain and the coefficient of performance of the cell.

Keywords: Hydrogen recovery; Hydrogen purification; Hydrogen compression; Electrochemical compressor

1. Introduction

Numerous studies on future energy development forecast hydrogen as energy storage or energy vector. There are two fundamental ways for using energy: stationary or mobile. While the stationary use does not exhibit any particular problem and can be performed in a well-controlled way, peculiar aspects are present when energy is used in a moving equipment.

A vehicle may go on a fixed route, such as a train, a tramway, etc., or on a free path. In the first case energy may be supplied along the route, such as, for instance, with an electric cable, in the second case energy must be stored on board and must have a high energy density either referred to the mass or to the volume; gasoline offers the best performance.

The large diffusion of personal cars in urban areas, fed with gasoline, raises air pollution over any acceptable level, and this may cause stops of urban traffic. A possible solution is the use of low polluting or no polluting engine and fuel (zero emission vehicles, ZEV). Actually the best solution found is the use of hydrogen as a fuel and the fuel cell as engine.

There is no doubt that, from a theoretical point of view, hydrogen appears to be the best non-polluting fuel, but, from a practical point of view, for its extended use some remarks must be pass.

Production of hydrogen is still an energy expensive process, mainly if renewable energy sources are used: the exergy yield is in the range 50–70% using fossil energy and 30–50% using renewable energy. Hydrogen compression (200–600 bar), or liquefaction (−253 °C, 2 bar), and distribution need about one half of the exergy content of the hydrogen itself.

If one disregards the economical aspects, which however are relevant for any human activity, but only the thermodynamic aspects are considered, the exergy balance in hydrogen production process and distribution is a milestone in the direction of a large diffusion of hydrogen as energy vector or energy storage. In the light of these facts any research in the direction of increasing the exergetic efficiency of hydrogen production and/or distribution is welcome.

Recently all electrochemical processes, as non-thermal processes, involved in hydrogen production and utilization have been investigated with the aim of increasing their efficiency.

* Corresponding author.
E-mail address: luciano.zanderighi@unimi.it (L. Zanderighi).

0378-7753/$ – see front matter © 2008 Elsevier B.V. All rights reserved.
doi:10.1016/j.jpowsour.2008.01.096

Nomenclature

D	diffusion coefficient
E	cell voltage
E_{rev}	reversible (Nernstian) cell voltage
f_H, f_e	specific hydrogen rate across the membrane
F, F_H	feed rate, of hydrogen
i, i^{eo}	current density
I	current intensity
Δp_i	pressure difference of gas between cathodic and anodic compartment
P_H, P_N	permeability, of hydrogen or nitrogen
r	ratio between water and hydrogen moles in the feed
R	gas constant
S	membrane surface area
T	temperature
x_H	hydrogen mole fraction in the feed

Greek letters

α	electro-osmotic drag
Ω	ohmic resistance
$\Im$	Faraday constant

Presently good results have been achieved with high-pressure electrolysis of water: electrolysis cells for the production of hydrogen at 100 atm are commercially available and cells for the production of hydrogen at 200 atm are under study. With these cells hydrogen production and compression are performed in one step with a significant saving in terms of investment costs and of exergy consumption in the compression stage.

Other researches have applied the electrochemical principle to the compression [1–4] or purification [5–7] of hydrogen: while in a fuel cell hydrogen and oxygen are fed, respectively, to the anodic and the cathodic compartment in order to produce electric energy, in a purification/compression system electric energy is supplied to the cell for transporting hydrogen from the anodic to the cathodic compartment through a mechanism that involves the oxidation of hydrogen in the anodic compartment with formation of protons, the transport of protons through a proton-conducting membrane, and their reduction in the cathodic compartment with formation of molecular hydrogen. Since any concentration/purification process is a compression process, from low to a high partial pressure, up to the pressure of the pure component, the minimum electrical work to be supplied to the cell is the theoretical work of compression as described by the Nernst equation.

In the present work we have investigated some fundamental aspects in the electrochemical concentration/purification of hydrogen such as

- gas distribution plates and related fluid-dynamics;
- gas flow rate in the electrode compartment;
- electrochemical procedure: galvanostatic or tensiostatic;
- role of water;
- coefficient of performance of the process;
- exergetic gain of the electrochemical process.

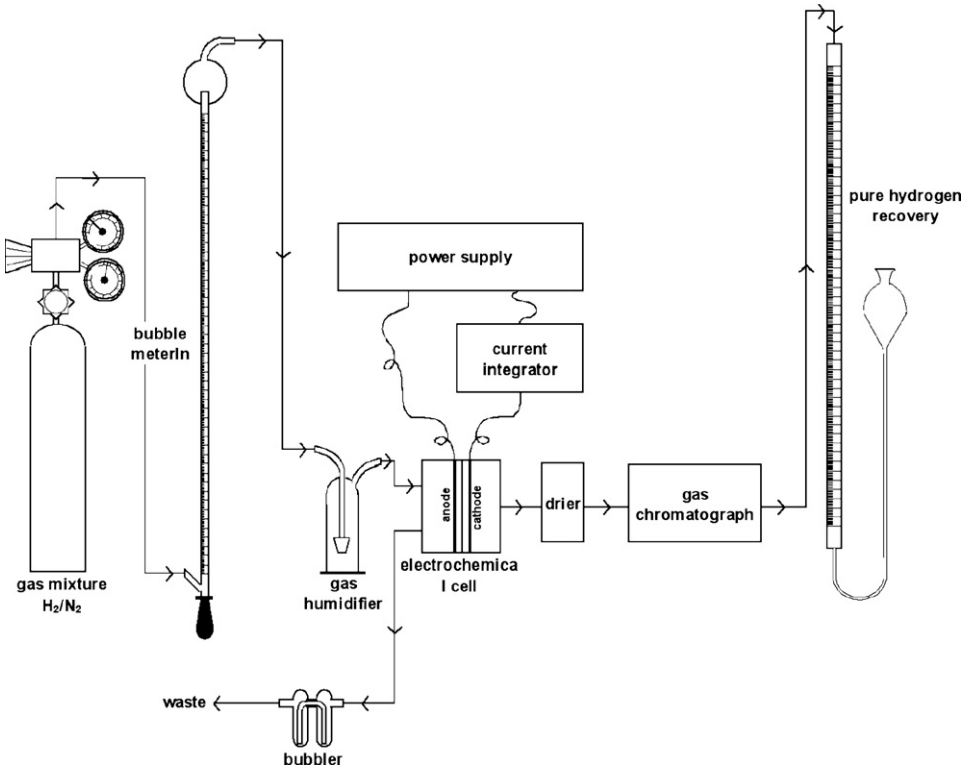

Fig. 1. Drawing of the experimental set-up.

2. Experimental

2.1. Experimental set-up

The experimental set-up is shown in Fig. 1. A gas mixture, 90% nitrogen, 10% hydrogen, flows from a cylinder to a bubble metering, a gas humidifier and finally to the anodic compartment of the electrochemical cell. The hydrogen produced in the cathodic compartment is collected and measured in a graduated burette over distilled water, due correction being made for the water partial pressure. The gas humidifier and the cell may be heated in the range 298–343 K, in a heated box, in order to change the partial pressure of water vapour in the gas delivered to the cell. Direct current was supplied by a power supply (AMEL mod 2055); a current integrator (AMEL model 721, range 0–19,980 C) was used to get the amount of the electric charge in a test run. The GC analysis of the cathodic exit stream allows evaluating the purity of produced hydrogen.

2.2. Electrochemical cell

The schematic exploded view of the electrochemical cell is shown in Fig. 2. The cell is composed of two end plates (in plexiglas or in stainless steel) to assemble the cell, two graphite or stainless steel plates with gas flow channels, two porous activated graphite electrodes, a proton-conducting membrane, appropriate silicon gaskets.

In order to study the fluid dynamics of the system, two symmetrical gas distribution plates with different flow channel path, were designed (Fig. 3). The first type has 21 parallel channels (0.2 cm × 0.1 cm; 5.7 cm length each), connected to two distribution channels; the mean path of the feed in the distribution plate is 6.85 cm; the total volume of the gas distribution channels is 2.88 cm^3. The second type of gas distribution plates has a single zigzag-shaped channel (0.2 cm × 0.2 cm, total length 137 cm) and its volume is 5.48 cm^3. In both cases the membrane electrode assembly (MEA) has a surface of 50 cm^2.

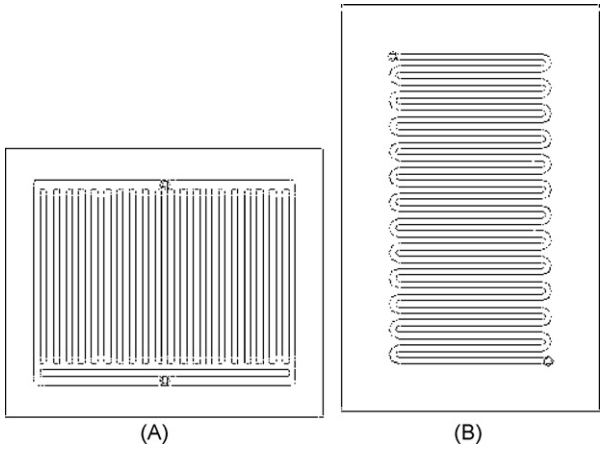

Fig. 3. The two different designs of the gas distribution plates: (a) 21 parallel channels and (b) a single long zigzag channel.

2.3. Membrane electrode assembly

The proton-conducting membrane was commercial Nafion 117, activated before use. The graphite electrodes had 10 g m^{-2} of Pt as catalyst. The membrane and the electrodes (MEA) were assembled in the cell without previous treatment since our aim was to study some fundamental aspects in hydrogen compression/purification and not to optimize the MEA.

2.4. Test runs

The test runs were planned in order to study:

- Cell-operating mode: it is possible to operate under galvanostatic or tensiostatic control. In the first case one measures the cell voltage (driving force) for an assigned current density

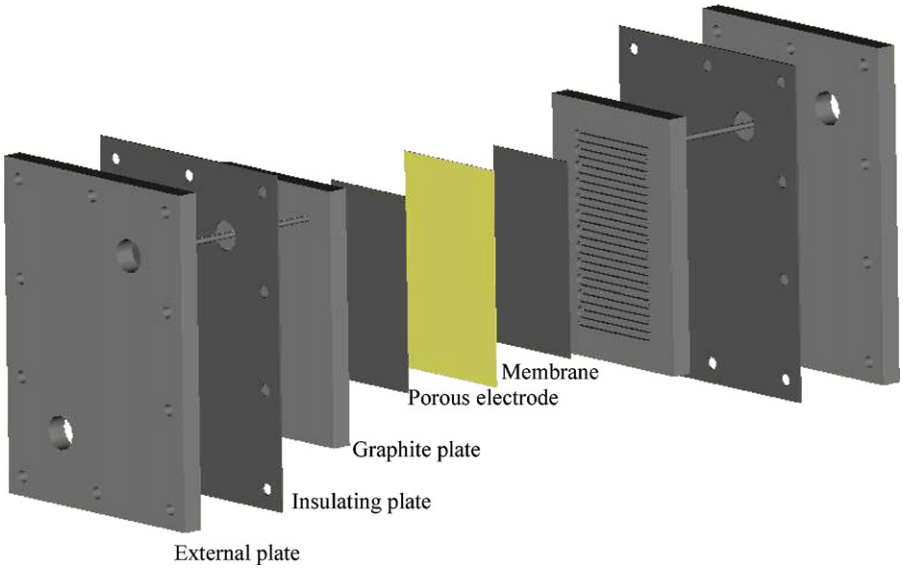

Fig. 2. Exploded view of the assembled purification/compression PEM-cell.

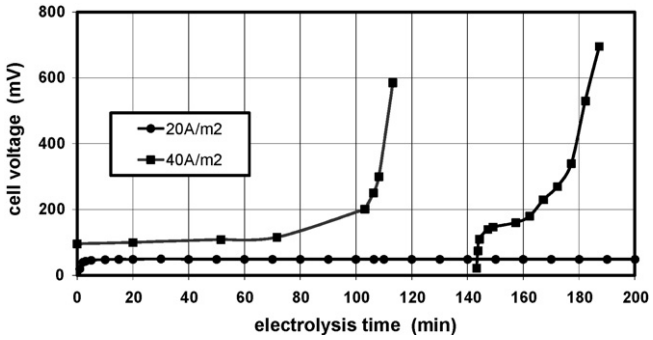

Fig. 4. Cell voltage vs. experimental time under amperostatic conditions ($i = 20$ and 40 A m^{-2}, $T = 298$ K, feeding flow = 18.0 N ml min^{-1}).

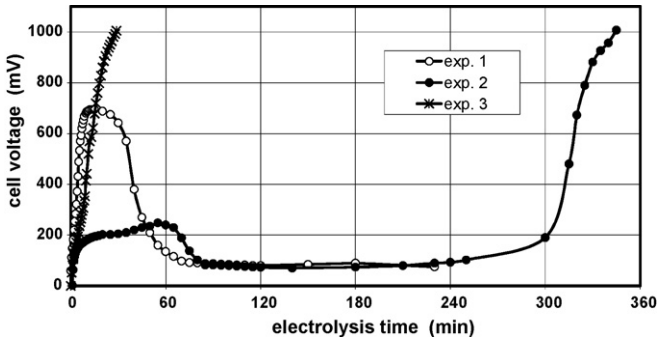

Fig. 5. Three replicated runs under amperostatic conditions ($i = 20$ A m^{-2}, $T = 318$ K, FFR = 11.4 N ml min^{-1}). Cell voltage vs. experimental time for first (Exp1), second (Exp2) and third (Exp3) runs in sequence. A non-reproducible behaviour has been observed.

(rate of the process), which is related to the rate of hydrogen production in the cathodic compartment; in the second case one measures the current density for a given value of applied voltage. In other words, with galvanostatic conditions, the rate of the process is assigned and the driving force is measured; under tensiostatic conditions the driving force is assigned and the rate of hydrogen production is measured.

- Role of water: high ionic conductivity of the proton-conducting membrane can be preserved only if the membrane is in hydrated form. In fuel cells, generally, humid hydrogen is fed into the anodic compartment while in the cathodic compartment, the water transported by protons across the membrane and that formed by reaction with oxygen accumulates and, at least in part, diffuses from cathodic to anodic compartment across the membrane. Therefore, in stationary conditions, the membrane has always a high degree of humidity, and water must be removed from cathodic compartment to prevent flooding. In a compression/purification cell water must be added to the cathodic compartment to preserve the optimal hydration degree of the membrane and to provide a suitable reserve for water saturated hydrogen outflow.
- Gas flow rate in the anodic compartment: the flow dynamics of the system can influence, through the hydrogen concentration gradient, electrode polarization and/or water need, not only the electrochemical parameters such as cell resistance and current intensity, but also the fraction of recovered hydrogen. At high flow rates there might be no concentration polarization but the fraction of recovered hydrogen could decrease dramatically.

3. Results

3.1. Galvanostatic measurements

Initial test runs were performed under galvanostatic conditions at the temperature of 298 and 333 K; the current density was 20, 40 and 60 A m^{-2}; the feed flow rate was in the range 6.5–19.0 N ml min^{-1}. In Fig. 4 a typical behaviour of the cell ($i = 20$ and 40 A m^{-2}; $T = 298$ K; $F = 18.0$ N ml min^{-1}) is reported: with $i = 40$ A m^{-2} the cell voltage increases over any acceptable values. If the run is restarted after the current has been interrupted for a while (e.g. 30 min) the E vs. time plot is the same as before, but the increase of voltage occurs earlier.

By using lower values of current density ($i = 20$ A m^{-2}) (Fig. 4) it is possible to obtain a stationary value of the voltage, at least for high values of the feed stream, but if the stream flow is decreased the voltage becomes unstable again.

After many runs we hypothesized that this behaviour is due to the dehydration of the membrane and decided to partially flood with water the gas flow channels in the cathode compartment, with the aim of getting a constant degree of humidity inside the membrane. Actually no improvement has been obtained, but a schizophrenic behaviour was observed (see for instance Fig. 5).

Summarising these results it is possible to say that stable-operating conditions can be obtained with low values of current density and high values of the feed flow rate (FFR). At the temperature of 343 K stable-operating conditions can be obtained at higher current densities ($i = 40$ A m^{-2}) but always with high FFR (>20 N ml min^{-1}).

3.2. Tensiostatic measurements

Following the hypothesis that time instabilities of the cell under galvanostatic conditions are due to the lack of hydration water for some assigned value of transfer rate of protons, we decided to perform test runs under tensiostatic conditions. With these operating conditions, when there is not sufficient water in the feed to hydrate all protons, a dehydration of the membrane occurs which causes an increase of the membrane resistance, a decrease of current, and therefore, the system self-regulates. In order to get current densities as high as possible, the cathode compartment was maintained always partially flooded, just to assure a suitable reservoir of water not only to hydrate the membrane but also to saturate the hydrogen exiting the cathodic compartment.

3.2.1. Tensiostatic runs with parallel channels in the distribution plates

The runs were performed at 298 and 343 K; the FFRs were in the range 4–80 N ml min^{-1}; the applied voltages were 35, 50, 100, and 150 mV.

3.2.1.1. Tensiostatic runs at 298 K. Typical trends of current density vs. time for various values of FFR are reported in

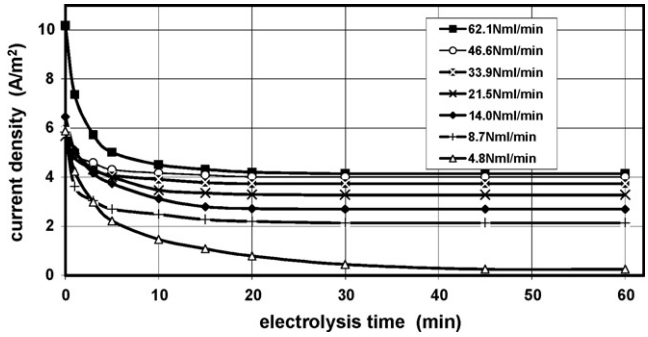

Fig. 6. Current density vs. experimental time under tensiostatic conditions (cell voltage = 35 mV, T = 298 K), for various feed flow rate.

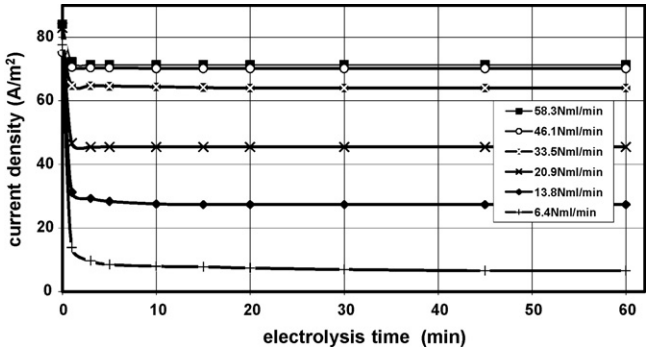

Fig. 7. Current density vs. experimental time under tensiostatic conditions (cell voltage = 150 mV, T = 298 K), for various feed flow rate.

Figs. 6 (E = 35 mV) and 7 (E = 150 mV): after an initial transition period, that may last about 30 min, stationary values of the electric current are reached; the value of the stationary electric current increases with FFR. Moreover, the increase of current density is high for low values of the FFR and rises to a limit value for high FFR.

Fig. 8 shows the hydrogen recovery fraction (i.e. the ratio recovered hydrogen/total hydrogen fed with the gas mixture, under stationary, i.e. constant current, conditions) vs. FFR for different values of the applied voltage. At low applied voltages (35 and 50 mV) the fraction of recovered hydrogen decreases by increasing the FFR; at high-applied voltages (100 and 150 mV) a maximum in the recovered hydrogen fraction is present at

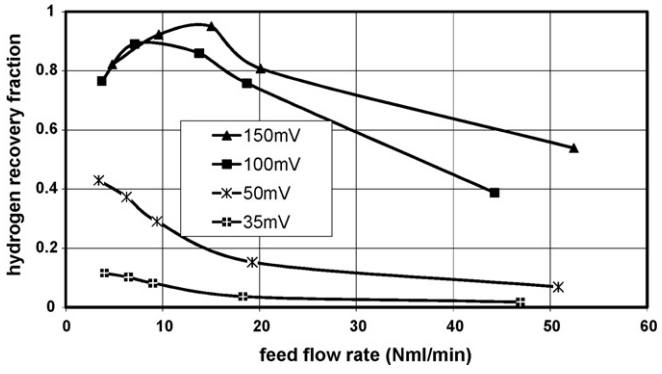

Fig. 8. The hydrogen recovery fraction vs. the feed flow rate (T = 298 K) under tensiostatic conditions (cell voltage 35, 50, 100, 150 mV).

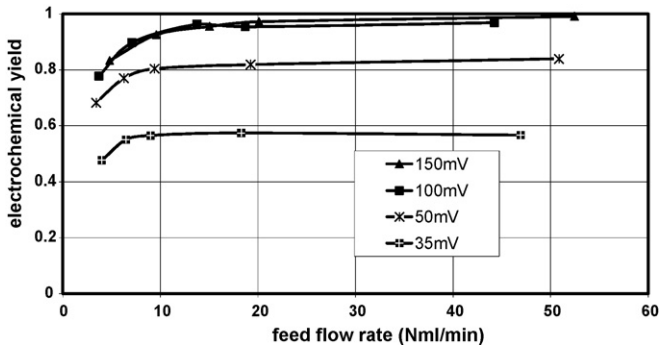

Fig. 9. The electrochemical yield vs. the feed flow rate (T = 298 K) under tensiostatic conditions (cell voltage 35, 50, 100, 150 mV).

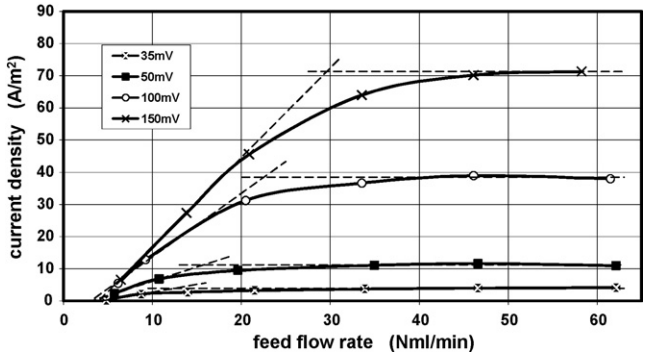

Fig. 10. The stationary current density versus the feed flow rate (T = 298 K) under tensiostatic conditions (cell voltage 35, 50, 100, 150 mV).

low FFR values (the maximum of hydrogen recovery is at 5–10 N ml min^{-1} for E = 100 mV and 10–15 N ml min^{-1} for E = 150 mV). Probably, at low applied voltages, the maximum of hydrogen recovery could be present at FFRs lower than the tested values.

The electrochemical yields (produced hydrogen/theoretical hydrogen, evaluated on the basis of transferred charge) vs. FFR, for different values of applied voltage, are shown in Fig. 9.

For all voltages the electrochemical yield increases with FFR up to a limit value, and this limit value increases with the applied voltage.

In Fig. 10 the stationary current values for all applied voltages as a function of FFR are plotted. For all voltages an increase of stationary current values is observed for low values of FFR, while for high FFR limit values of stationary current are reached and these limit values increase with the applied voltage.

3.2.1.2. Tensiostatic runs at 343 K. The runs performed at 343 K have a trend similar to that ones performed at 298 K, but the fraction of recovered hydrogen and the electrochemical yield are lower at 343 K than at 298 K.

3.2.2. Tensiostatic runs with a single zigzag channel in the distribution plates

The runs were performed at E = 100, 150 and 200 mV; the FFR was in the range 4–65 N ml min^{-1}. With the aim of verifying the presence of hysteresis phenomena the FFR was increased from the starting value up to the maximum value and then

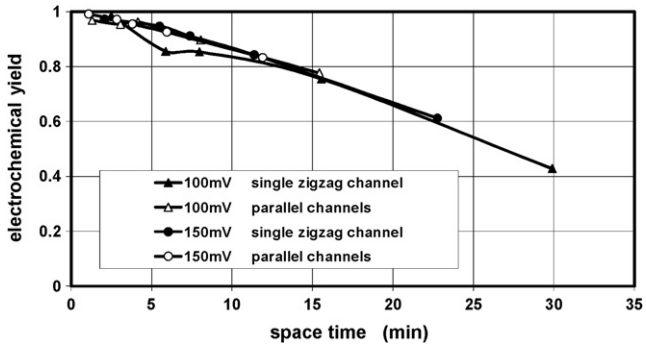

Fig. 11. The electrochemical yield vs. space time for the two types of the gas distribution plates (cell voltage = 100 and 150 mV; $T = 298$ K).

decreased to the initial value. The measured current intensity in the up and down runs was within the range of the experimental error, thus indicating that no change in the cell performances occurs during the test runs. As in the runs with parallel channels a transition time up to 30 min is present before a stationary value of current intensity is reached, also the plots of the intensity vs. FFR are similar and the previous comments hold.

A comparison between the two types of distribution plates, with different gas path and inner volume, can be made in term of hydrogen space-time instead of FFR. The electrochemical yields and the hydrogen recovery fraction at 100 and 150 mV for both types of channels vs. space time are shown in Figs. 11 and 12, respectively: in both cases the general trend is the same but parallel channels show slightly higher hydrogen recovery except for low values of space time.

3.3. GC analysis of hydrogen outflow

The analysis of the cathodic hydrogen stream has revealed the presence of oxygen and nitrogen. Actually oxygen is present in a small amount with respect to nitrogen and, most probably, it comes from ambient air through the gaskets or some very small leakage. The excess of nitrogen, with respect to the one from air as evaluated on the basis of oxygen, must be assigned to some nitrogen crossover from anode to cathode. In Fig. 13 the mean values of excess nitrogen concentration vs. current density at 298 K are reported.

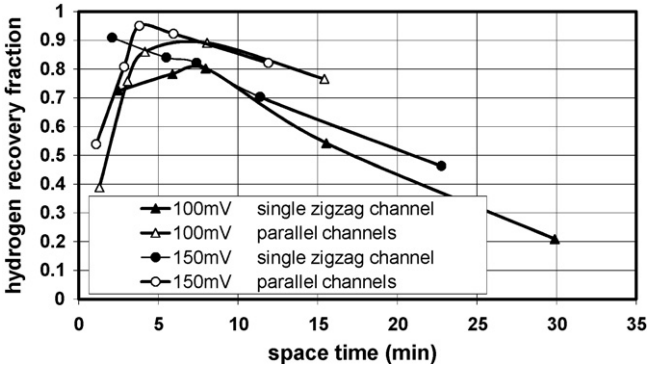

Fig. 12. The hydrogen recovery fraction vs. space time: different performances of the two different shapes of the gas distribution plates (cell voltage = 100 and 150 mV; $T = 298$ K).

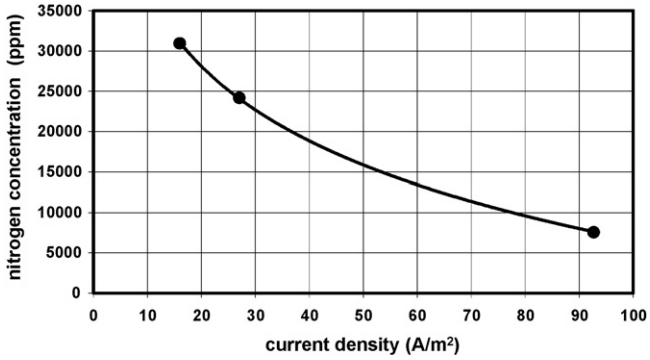

Fig. 13. Ppm of nitrogen in the cathodic hydrogen vs. current density at 298 K.

4. Discussion

Before any analysis of the experimental results is performed, it is important to discuss three fundamental aspects:

- mass transfer and fluid dynamics;
- role of water in proton transfer;
- the role of crossover flows.

4.1. Mass transfer and fluid dynamics considerations

As described previously two different feed flow paths have been used: 21 parallel channels or a single zigzag channel. The feed rate in the square channels was in the range 0.05–1.1 $cm^3\,min^{-1}$; the evaluated Reynolds number has the maximum value of 2.55, this means that the flow in the channels is always laminar.

Since the two feed distribution plates have different gas volumes, the space-time is different for equal flow rate.

It is possible to make a rough evaluation of the diffusion rate of hydrogen in the direction of the polymer membrane in presence of a laminar flow. The data used are

hydrogen diffusion coefficient in nitrogen $D = 0.41\,cm^2\,s^{-1}$;
diffusion path equal to the channel thickness (0.1/0.2 cm);
hydrogen concentration in the feed $3.93 \times 10^{-6}\,mol\,cm^{-3}$ (molar fraction in the stream 0.1);
hydrogen concentration at the exit $4.32 \times 10^{-7}\,mol\,cm^{-3}$ (molar fraction in the stream 0.011; assuming a recovery of 90%).

Since the transport of nitrogen through the MEA can be neglected with respect to its flow rate, the hydrogen diffusion in gas phase can be studied using a diffusion model of hydrogen in stationary nitrogen. The hydrogen diffusion flow rate results to be $1.76 \times 10^{-5}\,mol\,s\,(cm^2)^{-1}$ in the feed mixture, and $1.68 \times 10^{-6}\,mol\,s^{-1}\,(cm^2)^{-1}$ in the exit mixture.

If one assumes that all the diffusing hydrogen is transported across the membrane the current density ($A\,m^{-2}$) that can be obtained results in the range 32–34 ($kA\,m^{-2}$); these values are some order of magnitude greater than the measured experimental values, therefore it is possible to exclude that the process under study is limited by hydrogen mass transfer in the gaseous phase.

4.2. The role of water in proton transfer

It is known from PEM fuel cells that the proton conductivity of the polymer membrane strongly depends on the hydration of the membrane. Moreover, protons cross the wetted membrane with at least three hydration molecules. The experimental test runs have shown that:

- in the humid feed the molar ratio H_2O/H_2 is 3, 1/10, while to transport hydrogen across the Nafion membrane the ratio has to be around 60/10 (three molecules of water for one proton);
- it is not sufficient to saturate the feed with water: the cathodic compartment must be partially flooded in order to hydrate the membrane and to get stable behaviour and reproducible results;
- galvanostatic procedure operates only with low values of the current: high current values induce an increase of voltage as a consequence of the decrease of hydration of PEM due to high flow of hydrate protons. With tensiostatic procedure the system self regulates and the flow of protons, that is current density, reaches a stationary value consistent with the hydration degree of the membrane. Actually in all tensiostatic runs an initial transition period has been observed in which the current density decreases before reaching a stationary value related to a stable state of hydration of the membrane.

The feed stream is saturated with water at 298 or at 343 K; the molar ratio r between the water and the hydrogen moles is 0.32 at 298, and 1.39 at 343 K. Assuming the water vapour available in the feed is the limiting factor for proton hydration, which means that the amount of water in the feed is the limiting factor for the transfer of hydrated protons from anode to cathode, the maximum current intensity should be

$$i^{eo} = \frac{F_{x_H} r}{S\alpha}(2\Im) \quad (1)$$

where F_{x_H} is the hydrogen feed, S the surface area of the electrode, and α is the electro-osmotic drag coefficient. From the literature [8] α is in the range 0.1–0.6.

For instance, at 298 K, $r = 0.32$, the maximum current density is

$$i^{eo} = \frac{F_H \times 0.32 \times 96480 \times 2}{\alpha \times S \times 60 \times 22400} = \frac{4.6 \times 10^{-2} \times F_H}{\alpha \times S} \quad (A/m^2) \quad (2)$$

F_H (ml min^{-1}); S (m^2).

Actually, in the test runs the stationary current has higher values (about 10 times) and depends on the applied voltage. Therefore, the proton transfer is not limited by water content in the feed, and thus one must conclude that the water diffusion from cathodic to anodic compartment across the membrane has a relevant role: the combination of applied voltage and of membrane hydration defines the value of the stationary current with a sort of self-regulating mechanism, which allows getting a sufficient hydration of Nafion.

4.3. Nitrogen and hydrogen crossover

From the GC analytical data of hydrogen outflow a mean value of permeation coefficient, based on the thickness of Nafion 117, can be evaluated: $P_N = (6 \pm 1) \times 10^{-15}$ mol s^{-1} (mPa)$^{-1}$. This value agrees quite well with data reported in the literature [9,10].

The difference between the theoretical hydrogen production, evaluated on the basis of the measured electric current ($F_H^{th} = I/2 \times F$ mol s) and the experimentally collected hydrogen, allows to evaluate the hydrogen crossover from cathode to anode. The averaged value on at least 50 experimental data is $P_H = (5.5 \pm 2) \times 10^{-14}$ mol s^{-1} (mPa)$^{-1}$; this value is consistent with literature data [10].

4.4. Feed flow rate (FFR), applied voltage (V) and electric current (I)

In Fig. 10 the results of the runs at 298 K are summarized; similar plot has been obtained with the runs at 343 K: since no significant differences have been found between the two types of distribution plates the mean data of current density vs. FFR are plotted. For a given applied voltage the current density increases linearly at low value of FFR, but, at high values, the current density reaches a limit value, independent from FFR but dependent on the applied voltage. The analysis of the data at 298 and 343 K suggests that, for low FFR, the electric current is limited by hydrogen fed; at high FFR the electric resistance of the cell limits the process. By extrapolating the linear part of the plot until intersecting the line of the electric current limit value one obtains the point where the density of the electric current equals the limit current of the cell. The corresponding FFR is the theoretical maximum FFR (TMFFR) for the applied voltage.

The cell voltage is the sum of the following terms:

$$E = E_{rev} + \eta_{c.t.} + \eta_{m.t.} + I\Omega \quad (3)$$

$E_{rev} = (RT/z\Im)\ln(p_c/p_a)$ is the Nernst thermodynamic potential (in our case about 30 mV); $\eta_{c.t.}$ the sum of the anode and the cathode charge transfer overpotentials (which have a logarithmic dependence on the current density), $\eta_{m.t}$ the mass transfer overpotential (i.e. the concentration polarization), and $I \times \Omega$, are so called ohmic drop, is the resistance offered by the cell to the transport of hydrogen ions towards the cathode. In this term one should include the ionic membrane resistance, the contact resistance and, but in a very complicated way, the ohmic drop due to H^+ transport across the porous electrode, a transport that takes place along the path provided by Nafion nanoparticles, a component of the porous electrode. By considering the current densities in our test runs and the high exchange current for the system H^+/H_2 on platinum black, the term $\eta_{c.t.}$ can be safely disregarded in the voltage balance (3). The term $\eta_{m.t.}$ could be a major component at low FFR (see Fig. 10) but can be acceptably neglected at high flow rate. The validity of this approximation is confirmed by the linearity of I vs. $E - E_{rev}$ at high flow rate (Fig. 14). As a consequence, at high FFR the previous equation

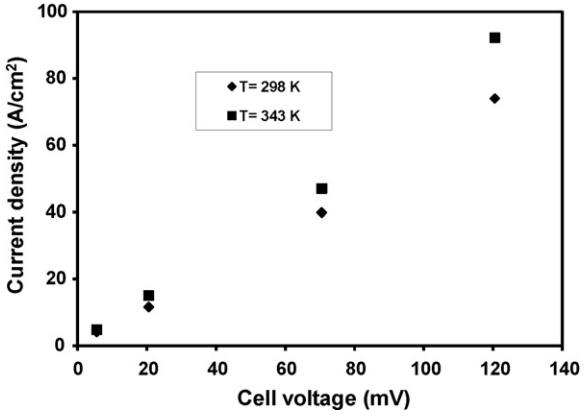

Fig. 14. Limit current density vs. applied voltage at 293 and 343 K.

(3) approximates to:

$$E \cong E_{\text{rev}} + I\Omega \tag{4}$$

from which it is possible to evaluate Ω, that is the cell resistance.

In Table 1 the TMFFR, the limit electric current and the cell resistance, evaluated according to the previous equation, are reported.

Since the conductivity at 298 K of a Nafion 117 membrane is 0.1 S cm^{-1} the resistance of the Nafion membrane in the used cells should be 3.5×10^{-3} Ω, that is about 100 times lower than the total resistance of the cell. As said the assembled MEA was made without any particular care and the resulting resistance is high. As it will be shown later a particular care must be devoted to the reduction of the total resistance of the cell.

4.5. Characterization of the electrochemical process

Four parameters must be considered in the electrochemical hydrogen purification/compression.

4.5.1. Hydrogen yield

Hydrogen yield: defined as the ratio between the recovered H_r and the fed H_f hydrogen

$$\eta_H = \frac{H_r}{H_f} \tag{5}$$

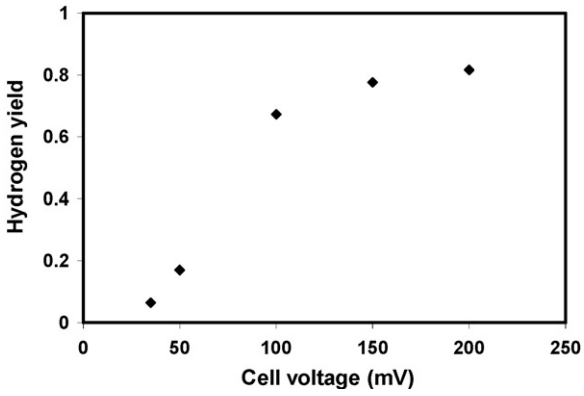

Fig. 15. Fraction of recovered hydrogen (hydrogen yield) vs. applied voltage.

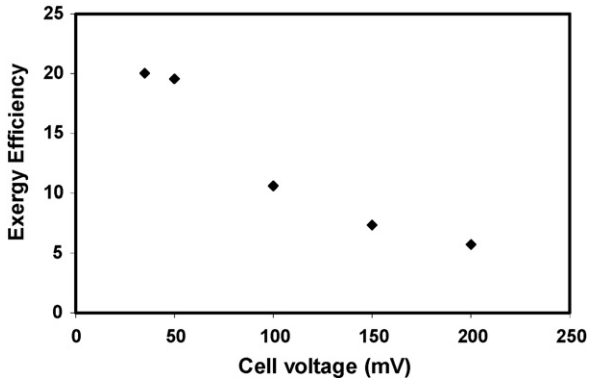

Fig. 16. Exergy efficiency vs. applied voltage at 298 K.

It is a measure of the fraction of recovered hydrogen. In Fig. 15 the hydrogen yield vs. the applied voltage is reported.

4.5.2. Exergy efficiency

Exergy efficiency: defined as the ratio between the exergy of recovered hydrogen and the exergy consumed in the production process

$$\varepsilon = \frac{H_r E_{x_{H_2}}}{IEt} \tag{6}$$

It is a measure of the work obtained with respect to the used electric work. The exergy efficiency vs. the applied voltage is reported in Fig. 16 at $T = 298$ K.

4.5.3. Coefficient of performance

Coefficient of performance: by assuming to feed a fraction of the produced hydrogen to a fuel cell for obtaining the power supplied to the process, the coefficient of performance of the process may be defined as the ratio between the hydrogen produced and the hydrogen consumed H_c in the fuel cell:

$$\mathbf{cop} = \frac{H_r}{H_c} \tag{7}$$

The greater the cop, the greater is the gain in hydrogen production with respect to the fraction of obtained hydrogen spent in a fuel cell to produce the used electric energy. Cop vs. applied voltage is reported in Fig. 17, at $T = 298$ K.

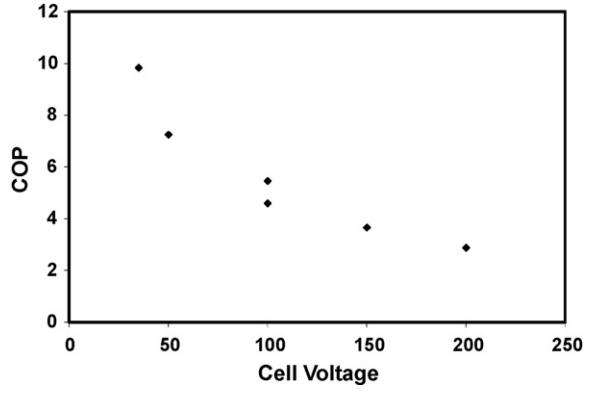

Fig. 17. Coefficient of performance (cop) vs. applied voltage at 298 K.

Table 1
Evaluation of the mean ohmic resistance of the cell

TMFFR	298 K			TMFFR	343 K		
MlH_2/min	I (mA)	$E - E_{rev}$(mV)	Ω (ohm)	mlH_2/min	I (mA)	$E - E_{rev}$ (mV)	Ω (ohm)
1.25	16	5.5	0.34	2.9	4	1	0.25
1.57	60	20.5	0.34	3.35	75	16	0.21
2.25	200	70.5	0.35	4.24	235	66	0.28
2.96	370	120.5	0.33	4.82	461	116	0.25
			0.34 (mean value)				0.25 (mean value)

Columns 1 and 5 the theoretical maximum feed flow rate (TMFFR) corresponding to the current intensity of columns 2 and 6 with the ohmic drop in columns 3 and 7. In columns 4 and 8 the calculated value of Ω, according to equation (4).

4.5.4. Cell efficiency

Cell efficiency: due to the difference in chemical potential between the cathode and anode compartments there is a mass transfer diffusion of molecular hydrogen across the membrane in the direction opposite to the proton transfer. The cell efficiency is defined as

$$\eta_{cell} = \frac{H_r}{H_p} \tag{8}$$

The produced hydrogen H_p is the hydrogen theoretically produced on the basis of current intensity:

$$H_p = \frac{I\,t}{(\Im \times 2)} \tag{9}$$

The η_{cell} vs. applied voltage at $T = 298$ K is reported in Fig. 18.

4.6. Current intensity, voltage and FFR

Either at 298 K or at 343 K the trend of the stationary (on the time scale) current intensity as a function of FFR for various voltages is the same: after a region of transition, where the current density increases, or decreases with FFR, a stationary current is obtained, and its value always increases with the applied voltage.

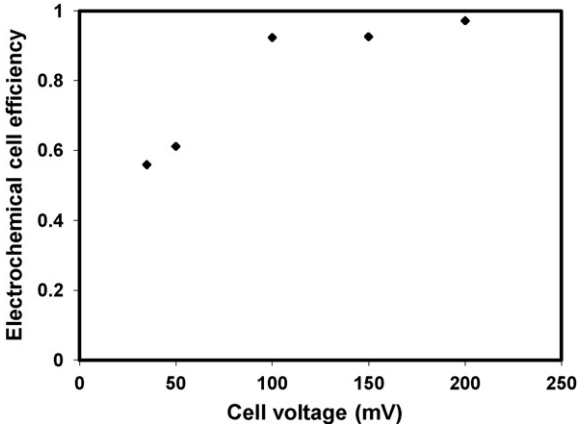

Fig. 18. Electrochemical cell efficiency vs. applied voltage at 298 K.

4.7. Applied voltage, hydrogen production and cross over flow

As previously discussed we preferred to work under tensiostatic condition, that is to fix the applied voltage and to leave the cell stabilize the current density:

$$i = \frac{E - E_{rev}}{S\Omega} \tag{10}$$

The specific hydrogen production rate (f_H) and the current density are related by the equation:

$$f_H = B \times i \tag{11}$$

where B is a dimensional constant ($B = 4.18 \times 10^{-4}$ (s m^3 (h C)$^{-1}$) for f_H (m^3 (m^2 h)$^{-1}$) and i (A m^{-2})).

The experimentally measured flow rate (f_e) of collected hydrogen takes into account the hydrogen and nitrogen crossover flow:

$$f_e = f_H + P_H\,\Delta p_H + P_N\,\Delta p_N \tag{12}$$

P_i is the permeation rate constant and Δp_i is the partial pressure differences with sign, between the anodic and cathodic compartment of the cell.

Since the crossover flows are independent from the electrical parameters, by increasing the current density the role of crossover flows decreases, that is, to increase the purity of hydrogen and the efficiency of hydrogen recovery the electric current has to be as high as possible.

From the previous equations (10)–(12) the hydrogen production rate results:

$$f_H = f_e - P_H\,\Delta p_H - P_N\,\Delta p_N = \frac{E \times B}{S \times \Omega} \tag{13}$$

The specific cell needs of electric power for hydrogen compression/separation (equation (4)) is

$$\boldsymbol{P} = i \times E = \frac{f_H\,[E_{rev} + (f_H/B)S\Omega]}{B} \tag{14}$$

$$\boldsymbol{P} = \boldsymbol{P}_T + \boldsymbol{P}_K \tag{15}$$

$\mathbf{P}_T = (f_H \times E_{rev})/B$ is the thermodynamic power need and $\mathbf{P}_K = (f_H/B)^2 \times \Omega \times S$ is the "kinetic" power need, or the power due to the driving forces against all resistances across the whole cell, such as electrode overpotentials and ohmic resistance.

The specific power consumption $\mathbf{P}_s = \mathbf{P}/f_H$ is

$$\mathbf{P}_s = \frac{E}{B} \tag{16}$$

For any cell the specific power consumption is a function of the applied voltage; the hydrogen production rate is a function of ratio between the applied voltage E and the cell resistance Ω. This is related to the cell resistivity ρ by the relation: $\Omega = \rho \times (l/S)$, where l is the thickness and S is the cross area of MEA, which is, by large, the main component of the total resistance.

To produce $1\,N\,m^3\,h^{-1}$ of hydrogen at 298 K, with an applied voltage of 0.15 V, the intensity of the current must be: $I = 2393$ A; the thermodynamic potential is $E_{rev} = 0.0295$ V; the driving potential, by neglecting the electrode overpotential, is $I \times \Omega' = 0.1205$ V, therefore the resistance of the cell is $\Omega' = 0.1205/2393 = 5.03 \times 10^{-5}\ \Omega$ and the MEA surface must be of $S = 33.8\,m^2$. The power consumption is $0.36\,kW\,h\,m^{-3}$.

For a specific hydrogen production rate, at a given applied voltage, the MEA resistivity determines the electrode and membrane surfaces, and, indirectly, the purity of hydrogen and the yield of production, since by increasing the MEA surface the crossflows both of hydrogen and nitrogen also increase.

4.8. Crossover effect

The crossover flows have a double effect: a decrease of both the yield of hydrogen production and the purity of produced hydrogen.

The fraction of lost hydrogen is

$$\xi = \frac{P_H S|\Delta p_H|}{BI} = \frac{|\Delta p_H|}{|\Delta p_H|_{lim}} \tag{17}$$

where $|\Delta p_H|_{lim}$ is the difference in hydrogen pressure between anode and cathode, corresponding to a crossflow equal to electrochemical hydrogen flow (for $\xi = 1$; $|\Delta p_H|_{lim} = B \times (I/S)/P_H$; $|\Delta p_H|_{lim}/E = (B/P_H)/(S \times \Omega)$). The residual fraction χ of hydrogen is

$$\chi = \frac{1 - \xi = 1 - [P_H|\Delta p_H|S\Omega]}{B \times E} \tag{18}$$

This result explains the data reported in Fig. 15: an increase of the voltage increases the yield of hydrogen, and therefore of the cell efficiency.

The fraction of nitrogen impurity present in the purified hydrogen and due to crossover flow is

$$\zeta = \frac{P_N S \Delta p_N}{B \times I + P_H S|\Delta p_N|} = \frac{\Delta \Pi_N/|\Delta p_H|}{(B/P_H|\Delta p_H|)(I/S) + P_H/P_N} = \frac{P_N\,\Delta p_N}{P_H|\Delta p_H|}\left(\frac{\xi}{1+\xi}\right) \tag{19}$$

The last equation relates the fraction of lost hydrogen with the fraction of nitrogen impurity.

4.9. Hydrogen recovery fraction

The recovered fraction is defined as

$$\varepsilon = \frac{f_H - P_H S|\Delta p_H|}{F x_H} \tag{20}$$

The maximum value of ε corresponds to $F_{x_H} = f_H$, which is all the hydrogen fed that can be transported by the applied voltage. By decreasing F also f_H decreases (its maximum value equals the fed hydrogen) and the crossover hydrogen flow may become significant: a decrease of hydrogen-recovered fraction occurs. This phenomenon is illustrated in Fig. 12. At high value of feed stream $F_{x_{H_2}} \gg f_{H_2}$, that is low value of space time (the value of $f_H = B \times I$ is constant), the recovered fraction decreases with space time.

5. Summary of the results and conclusions

(a) Tensiostatic operating condition must be preferred to galvanostatic one, since the former allows a self-control of the process kinetics, according to the hydration condition of the membrane. On the contrary, by fixing the kinetic of the process, as it occurs under galvanostatic condition, the hydration degree of the membrane is out of control, and an erratic behaviour results.

(b) The shape of the distribution channels has no influence on the hydrogen purification/compression process, as long as the hydrogen diffusion rate in gas phase is greater than the transport rate of hydrogen across MEA, as in the present case.

(c) The feed flow rate has a significant influence on the fraction of recovered hydrogen. With hydrogen feed flow rate (low residence time) greater than the maximum flow rate across the cell membrane, the recovered fraction increases with the decrease of the feed flow rate; when the flow rate of hydrogen feed equals the flow rate across of the membrane, the fraction of the recovered hydrogen reaches the maximum: this maximum is defined by the production rate and the hydrogen crossover. By further decreasing the hydrogen feed, the value of flow across the membrane also decreases and may be, at maximum, equal to the feed, while the hydrogen crossover flow is constant. The result is that the fraction of recovered fraction decreases to 0.

(d) The specific energy consumption is a function only of the applied voltage.

(e) The applied voltage splits into three terms: thermodynamic potential, defined by the compression ratio of the hydrogen; driving or "kinetic" potential, that defines the flow rate across the MEA, and dissipative potential, due to the useless forces.

(f) At a given applied voltage, the MEA resistivity determines the membrane surface area, the fraction of lost hydrogen due to the crossover, and the purity of produced hydrogen.

Acknowledgment

The authors are pleased to acknowledge ZINCAR (Zero INpact CARbon) s.r.l., sponsor of the research.

References

[1] B. Rohland, K. Eberle, R. Ströbel, J. Scholta, J. Garche, Electrochim. Acta 43 (1998) 3841–3846.
[2] R. Ströbel, M. Oszcipok, M. Fasil, B. Rohland, L. Jörissen, J. Garche, J. Power Sources 105 (2002) 208–215.
[3] A.W. Ballantine, G.A. Eisman, R.L. Chartrand, N. Komura, I. Yamashita US 20,050,053,813.
[4] T.Y. H. Wong, F. Girard, T.P.K. Vanderhoek WO03/075379 A2.
[5] K. Onda, K. Ichikara, M. Nagahama, Y. Minamoto, T. Araki, J. Power Sources 164 (2006) 1–10.
[6] H.K. Lee, H.Y. Choi, K.H. Choi, J.H. Park, T.H. Lee, J. Power Sources 132 (2004) 92–98.
[7] G.E. Benson, A.W. Ballantine, J.W. Parks, W.J. Zielinski, E.T. White, R.A. Sinuc, US 20,040,058,209.
[8] T. Murahashi, M. Naiki, E. Nishiyama, J. Power Sources 162 (2006) 1130–1136.
[9] S.S. Kocha, J.D. Yang, J.S. Yi, AIChE J. 52 (2006) 1916–1925;
T. Sakai, H. Takenaka, E. Torikai, J. Electrochem. Soc. 133 (1986) 88–92.
[10] T.A. Zawodzinski Jr., J. Phys. Chem. 95 (1991) 6040.